

# Low-Intensity 10 kHz Spinal Cord Stimulation Reduces Behavioral and Neural Hypersensitivity in a Rat Model of Painful Diabetic Neuropathy

Dong Wang, Kwan Yeop Lee, Dongchul Lee, Zachary B Kagan, Kerry Bradley 

Nevro Corp, Redwood City, CA, 94065, USA

Correspondence: Kerry Bradley, Nevro Corp, 1800 Bridge Pkwy, Redwood City, CA, 94065, USA, Email [bradleykerry19@gmail.com](mailto:bradleykerry19@gmail.com)

**Background:** Low-intensity 10 kHz spinal cord stimulation (SCS) has been shown to provide pain relief in patients with chronic pain resulting from diabetic peripheral neuropathy (DPN). However to date, there have been no studies of 10 kHz SCS in animal models of diabetes. We aimed to establish correlative data of the effects of this therapy on behavioral and electrophysiological measures in a DPN model.

**Methods:** Twenty-five adult male Sprague-Dawley rats were injected once intraperitoneally with 60 mg/kg streptozotocin (STZ) to induce diabetes over a subsequent 4 w period, while 4 naïve control animals were not injected. After approximately 21 d, 12 of STZ-injected rats had mini epidural SCS leads implanted: 8 received continuous low intensity (~30% motor threshold) 10 kHz SCS, and 4 received sham SCS (0 mA) over 7 d. Behavioral assays (von Frey filament probe of hindpaw) were measured in 18 animals and in vivo dorsal horn electrophysiological studies (receptive field; response to afferent brush, von Frey probe, pinch) were performed in 17 animals.

**Results:** Across behavioral assays of mechanical allodynia and electrophysiological assays of receptive field size and mechanosensitivity, diabetic animals stimulated with 10 kHz SCS showed statistically significant improvements compared to sham SCS.

**Conclusion:** Low-intensity 10 kHz SCS produced several measures associated with a reduction of pain in diabetic rodent models that may help explain the clinical benefits of 10 kHz SCS in patients with painful diabetic neuropathy.

**Keywords:** animal model, spinal cord stimulation, neuromodulation, painful diabetic, 10 kHz, high frequency

## Introduction

Diabetic peripheral neuropathy (DPN) is the most common complication of diabetes mellitus.<sup>1</sup> A large cohort of patients with DPN (at least 20%) develop life-altering symptoms in their distal extremities, most commonly pain, numbness, paresthesia, and burning.<sup>2</sup> Pharmacologic treatment of painful diabetic neuropathy (PDN) (eg, gabapentinoids, SNRIs) is often only moderately successful, demonstrating large number-needed-to-treat estimates, significant side-effect profiles, and high rates of discontinuation.<sup>3–5</sup> Paresthesia-based spinal cord stimulation (SCS) has been attempted historically to treat diabetic pain, and has shown reasonable success in relatively small studies.<sup>6–9</sup> More recently, paresthesia-free 10 kHz SCS has been evaluated for chronic pain in diabetic patients and has shown excellent results as an adjunct to and compared to conventional medical management.<sup>10</sup>

The lack of stimulation-induced paresthesia with 10 kHz SCS suggests that dorsal column activation is not involved and thus mechanistically is different than traditional paresthesia-based SCS.<sup>11–13</sup> Preclinical work investigating low intensity (ie, ostensibly paresthesia-free) 10 kHz SCS in normal and spared nerve injury rodent models has suggested that several spinal mechanisms may be involved, eg, alteration of synaptic activity via glutamate transporter modulation, and selective activation of dorsal horn inhibitory interneurons in the dorsal horn.<sup>14,15</sup> Spinal mechanisms of 10 kHz SCS have not yet been explored in animal models of diabetes. To underscore the clinical findings of pain relief, we initiated

investigations into the behavioral and electrophysiologic effects of clinically relevant 10 kHz SCS in preclinical studies of diabetic model rodents.

## Materials and Methods

### PDN Model

All experimental procedures were carried out in accordance with the National Institute of Health Guide for the Care and Use of Laboratory Animals and approved by the Animal Care Committee at Explora BioLabs (San Diego, CA), protocol number EB20-016-001. All efforts were made to minimize the number of animals used and their suffering in this study.

The streptozotocin (STZ)-induced diabetic rat is the most commonly employed animal model used to study mechanisms of painful diabetic neuropathy.<sup>16,17</sup> A single effective dose of the cytotoxic agent STZ will cause rats to become hyperglycemic within 72 h. Injected rats will next exhibit behavioral signs consistent with the development of a painful neuropathy.<sup>18</sup> Generally, adult male Sprague-Dawley rats (7–8 w old; body weight ~ 250–300 g; Charles River Labs) were weighed, tail vein blood glucose (BG) was measured (Blood Glucose Monitoring System, CareTouch, New York), and the withdrawal threshold of the left hind paw was assessed using von Frey (vF) filaments (Semmes-Weinstein monofilaments, Stoelting Co., IL). Animals were then given a single intraperitoneal (IP) injection of STZ (60 mg/kg, in a 0.9% saline vehicle) after fasting for 12–18 h. One hour after injection, animals had free access to food and water. Post-injection, body weight and BG were measured every 7 d. Onset of experimental diabetes was confirmed when BG > 270 mg/dl and expected body weight gain distinctly slowed or halted post-injection.

### Chronic Lead Implantation

Rats were anesthetized with isoflurane (2.0% for induction and 1.5% for maintenance) in a flow of O<sub>2</sub>, placed in a prone position, and the hair on their back was shaved and prepared for sterile surgery. A midline incision of skin and muscle was made for access to the L3-L4 vertebral junction. A cylindrical 3-contact SCS lead (420 μm diameter, 1mm-long contacts, interspaced with 1 mm-long nonconductive polymers) was advanced rostrally in the epidural space so that the stimulating contacts were dorsally positioned over the L5-L6 spinal segments (innervating the left hind paw). The position of the contacts was confirmed by hindlimb muscle twitch evoked by electrical stimulation through the SCS lead. At the vertebral exit, the lead was anchored to the adjacent musculature with sutures to prevent displacement. The proximal end of the lead was subcutaneously advanced so that the connector end of the lead could be placed above the skin, through a small incision made around the cervical-thoracic junction. The skin was closed around the protruding connector with sutures and the dorsal part of a chronically worn vest (Lomir Inc., Malone NY) harness covered the area.

### Spinal Cord Stimulation

After successful PDN model development and SCS lead implantation, 10 kHz SCS was administered to one animal group (STZ+10kHzSCS) for 7 d. Using a modified clinical trial stimulator module (TSM; Nevro, Redwood City, CA) connected via custom interface cabling and a rotary commutator to the implanted lead, rats receive continuous 10 kHz SCS (10 kHz, 30 μs @ 30% motor threshold {MT}, 24 h/d, while resident in their home cages). At lead implant, and prior to initiation of SCS, the MT was measured by applying pulsed 10 kHz (30 μs pulse width) with 3 ms ON/2 s OFF and increasing the amplitude until twitching in the ipsilateral paw and/or paraspinal musculature was observed.

### Animal Groups

Animals were randomized into one of four groups: Naïve, STZ-Control, STZ+ShamSCS, and STZ+10kHzSCS, where each animal is considered an experimental unit. The naïve group received no STZ injection or lead implant. The three non-naïve animal groups were diabetic pain models, receiving the STZ injection and demonstrating diabetic symptoms of elevated blood glucose and weight stagnation. Naïve and STZ-Control animals were not outfitted or instrumented during

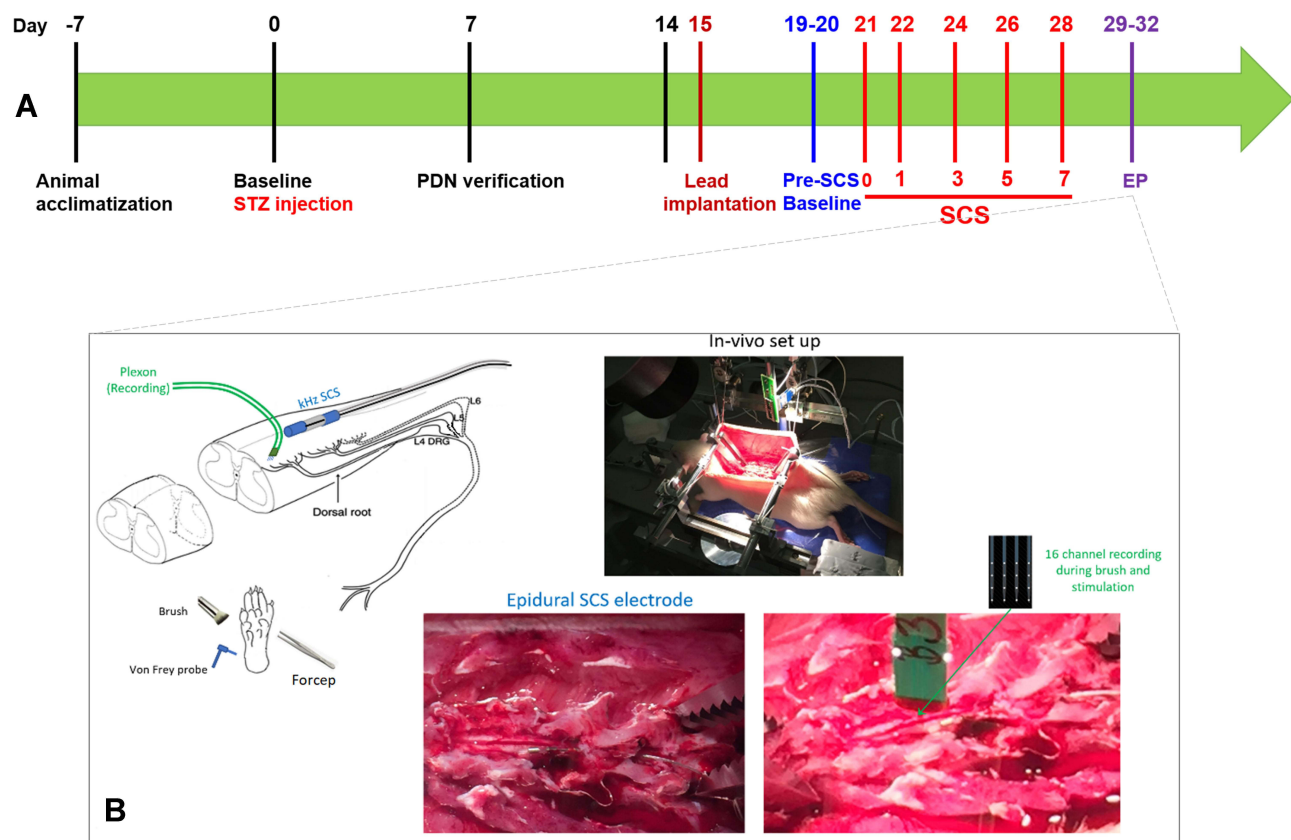


**Figure 1** Methodological aspects of study. **(A)** Graphical timeline of experimental procedures; **(B)** generalized in vivo electrophysiology experimental set up.

housing or experimentation. STZ+ShamSCS animals were not stimulated by the stimulator (device off) but retained all mechanical connections and tethering. No a priori explicit strategy beyond good scientific lab practice was employed to control experimental confounders.

## Behavioral Testing

The behavioral assay (mechanical sensitivity/allodynia) was performed using vF testing. The experimenter was blinded to the type of stimulation in the rats with implanted leads and to the STZ injection status of the non-instrumented rats. Behavioral assays were performed at Baseline/Day 0 (prior to STZ injection), Day 7, Day 14, Pre-SCS Baseline (Day 19–20), Day SCS0, Day SCS1, Day SCS3, Day SCS5, and Day SCS7 (Figure 1A).

To quantify mechanical hypersensitivity of the hind paw, rats were placed in individual plastic boxes on a mesh floor and allowed to acclimate for 30–45 m. A series of calibrated vF filaments (0.6, 1.0, 1.4, 2, 4, 6, 8, 10, and 15 g) were applied perpendicularly to the plantar surface of the hind paw with enough force to cause slight bending of the filaments. Brisk withdrawal or paw flinching within 4 s of filament application were considered as positive responses. In the absence of a response, the filament of next greater force was applied. In the presence of a response, the filament of next lower force was applied. The tactile stimulus producing a 50% likelihood of withdrawal was determined using an “up-down” calculating method.<sup>19</sup> Each trial was repeated two to three times at 2 m intervals, and the mean value was used as the withdrawal threshold. For linear statistical analyses, we converted the grams-Force of vF measurements using a log transformation.<sup>20</sup>

## In vivo Electrophysiology Testing

After Day 28 (the end of the STZ and SCS periods), electrophysiologic experimentation was performed using in vivo preparations (Figure 1B). We did not control for experimenter blinding in the electrophysiology measurements. Generally, after induction under isoflurane, anesthesia was maintained by regular doses of urethane (1.2 g/kg IP) which provides long-

acting anesthesia with minimal cardiovascular depression; this stability was essential for ensuring that we could finish long-duration electrophysiological experiments with adult male Sprague-Dawley rats. Body temperature was monitored by a rectal probe and maintained via a feedback regulated heating pad. Breathing and muscle tone were assessed throughout the experiment and additional urethane was administered if necessary. The back was shaved, the incision area prepared with Betadine, and an incision made so that the paraspinal muscles were separated from the spinous processes at the L1-S1 levels. With the paraspinal muscles retracted, a laminectomy was performed using standard techniques in order to expose the L5 spinal segment for recordings. The rat was placed in a stereotaxic frame using ear bars and vertebral clamps to secure the animal. In animals with previously implanted SCS leads, care was taken to gently dissect fibrous tissue surrounding the mini-sized SCS lead during the multi-level laminectomy. The SCS lead was then removed briefly while the dura mater was carefully excised, and the recording spinal area was prepared under microscopic vision. The SCS lead was then repositioned over the dorsal spinal cord, to the left of midline, just rostral to the L5 spinal segment. The MT was measured again after repositioning the lead to account for any changes. After MT was determined, micro-drivers were used to insert a 16-contact extracellular microelectrode array (NeuroNexus16ch, Ann Arbor, MI) into the lumbosacral enlargement of spinal dorsal horn, just proximal to the original position of the SCS electrodes. A small amount of mineral oil was placed over the electrode insertion sites.

We next determined the receptive field center of the dorsal horn neurons near the microelectrode recording array. Cells were predominantly located 500–800  $\mu\text{m}$  below the surface of the spinal cord, approximately located in Laminae III–V. Neurons were identified by their firing pattern response to brush and vF stimuli onto the ipsilateral hind paw. We excluded neurons that responded to limb displacement, indicating proprioceptive input. The signal was amplified, filtered at 500 Hz – 10 kHz, digitized at 40 kHz with an Omniplex Data Acquisition System and stored with stimulus markers on disk. Single units were isolated using Offline Sorter V3 software, and were analyzed with Neuroexplorer 5 (Plexon, Dallas TX). Electrophysiologic metrics included size and location of receptive field, and response of neurons to various afferent stimuli applied to the center of the receptive field on the left hind paw, as follows.

**Receptive Field:** Regions responsive to afferent probing by brush, blunt probes, or vF filaments to the glabrous skin of the left hind paw were mapped onto a generic image of the plantar surface of the paw. By using weak search stimuli, we targeted neurons receiving low-threshold input and avoided causing sensitization. Regions responsive to afferent probing were mapped onto a generic image of the plantar surface of the paw. GraphPad Prism (San Diego, CA) software was used to quantify the receptive field size for each animal and results were scaled and converted into square centimeter units.<sup>21–23</sup>

**Innocuous Brush** (small camel hair paint brush): a measurement spanned 20 s, during which 10 periods of “1 s of light (innocuous) brush then 1 s of no afferent stimuli” were applied to the paw ipsilateral to the SCS electrodes.

**von Frey Stimuli:** Five different vF filaments, ranging from innocuous to nociceptive forces (2, 6, 10, 25, and 60 g) were applied to the left hind paw (ipsilateral to the SCS electrodes). For 2–10 g filaments, vF was applied for 1 s, then withdrawn for a 1 s interval, a total of 10 times. An interval of 1 m without stimulation elapsed prior to applying the next filament. Since the 25 g and 60 g filaments were more intense stimuli, a 5 m “rest” period was implemented between the 25 g and 60 g filaments.

**Pinch (Bulldog clamp):** after an initial control period of 20 s, a firm pinch (ie, enough to generate pain in the hand of the experimenter) was applied for 1 s using a Bulldog clamp to the paw ipsilateral to the SCS electrodes. The response to pinch was the neural firing after discharge, recorded for 20–30 s following the pinch.

## Analysis

Summary statistics were calculated for continuous variables. Mixed model ANOVA was used to analyze the responses by group (treatment as fixed categorical factor) and by day of stimulation (fixed repeated factor). Log transformations to homogenize variances were employed in cases where Levene’s test indicated variances were unequal. Receptive field data was analyzed using a Means of Variance method (SPSS Statistics, IBM). Electrophysiologic data was analyzed using ANOVA with post-hoc Student’s *t*-test, or Kruskal–Wallis with post-hoc Nemenyi Q test, depending upon normality of the data assessed via Shapiro–Wilks test. Uncorrected differences with  $p < 0.05$  were considered significant (Real Statistics package, Microsoft Excel). Since there was no a priori hypothesis, sample sizes were determined by comparable studies in the literature and our early experience with the animal types evaluated.

## Results

### Disposition

For the behavioral work, we studied 29 rats; 25 were injected with STZ. Of those injected, 1 animal in the STZ+ShamSCS was euthanized during the behavioral portion of the study due to diabetic symptoms (ie, profound infection) and 4 others (2 in the STZ+ShamSCS, 1 in the STZ+10kHzSCS, and 1 in the STZ-Control groups) did not develop adequately elevated BG to be defined as PDN models (a priori threshold: BG  $\geq$  270 mg/dl). This allowed for 20 PDN-model animals, 12 of which had SCS leads. Eighteen (18) animals were dedicated for behavioral testing: STZ+10kHzSCS = 5; STZ+ShamSCS = 4; STZ-Control = 5; Naïve = 4. For electrophysiologic testing, 17 rats were used, 11 of which were drawn from the group undergoing behavioral testing, and six additional rats meeting the BG criteria above and instrumented/treated similarly to the behavioral groups: STZ+10kHzSCS = 6; STZ+ShamSCS = 3; STZ-Control = 4; Naïve = 4.

### Blood Glucose and Body Weight

Starting at Day 7, all PDN model animals in STZ-injected groups had ( $p < 0.01$ ) and maintained significantly elevated blood glucose compared to naïve animals (Day28/SCS Day 7: Naïve =  $165 \pm 14$ ; STZ+10kHzSCS =  $448 \pm 38$ ; STZ+ShamSCS =  $537 \pm 37$ ; STZ Control =  $471 \pm 43$  mg/dl;  $p < 0.001$ ; Figure 2). At all-time points, there was no statistical difference between the BG in the STZ-injected groups ( $p > 0.05$ ).

The change in body weight from Day 0 was compared for each group, with the Naïve animal group chosen as a reference (Figure 2). The increases in weight were significantly lower for the STZ+10kHzSCS ( $p = 0.0294$ ), STZ+ShamSCS ( $p = 0.0076$ ), and STZ-Control ( $p = 0.0027$ ) groups (Day28/SCS Day 7: Naïve =  $409 \pm 21$ ; STZ+10kHzSCS =  $346 \pm 15$ ; STZ+ShamSCS =  $341 \pm 8$ ; STZ Control =  $304 \pm 17$  g).

### Lead Implantation and Motor Thresholds

Leads were successfully implanted in 12 PDN-model animals. After leads were successfully implanted, on the Pre-Stim Baseline Day, in order to establish the chronic stimulation amplitude used in the study, motor thresholds were measured for animals in the STZ+10kHzSCS group. Mean MT thresholds across animals was  $0.34 \pm 0.03$  mA for 10 kHz, 30us. The stimulation amplitudes used in the study were set at approximately 30% of the individually measured MT for each animal.

### Behavioral

Mechanical Allodynia, von Frey Testing: Overall, compared to STZ+ShamSCS, the paw withdrawal thresholds were significantly higher in the Naïve ( $p < 0.0001$ ) and STZ+10kHzSCS ( $p = 0.03$ ) groups, while the STZ-Control was similar

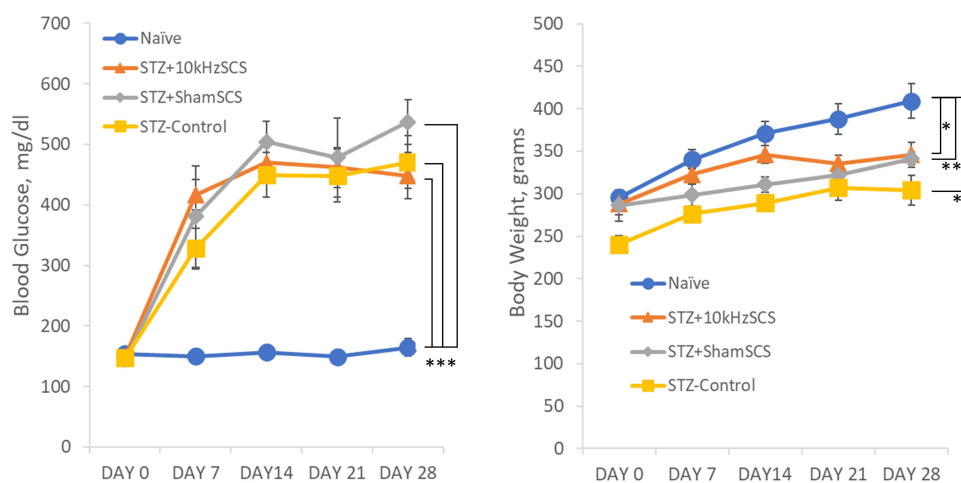


**Figure 2** Blood glucose and body weight measurements for each experimental group over time. \*  $p < 0.05$ ; \*\*  $p < 0.01$ ; \*\*\*  $p < 0.001$ .

to that of the STZ+ShamSCS group ( $p = 0.08$ ; Figure 3). After disease onset but prior to SCS initiation, compared to the STZ+ShamSCS group, the paw withdrawal thresholds from Pre-Stimulation were significantly greater for the Naïve ( $p = 0.007$ ) and STZ+10kHzSCS ( $p = 0.02$ ) groups, but not significantly different for the STZ-Control group ( $p = 0.62$ ). When compared to the Naïve group, all groups were significantly different (STZ+10kHzSCS:  $p = 0.0367$ ; STZ-Control:  $p = 0.0103$ ).

## Electrophysiology

**Receptive Field:** The mean receptive field area of dorsal horn neurons in the L5-L6 segments was significantly greater for the STZ+ShamSCS group than the areas of both the STZ+10kHzSCS ( $p = 0.0126$ ) and Naïve ( $p < 0.001$ ) groups, while not statistically different than the STZ-Control group ( $p = 0.1308$ ) (Figure 4).

**Mechanosensitivity, Brush:** Firing rates of dorsal neurons were significantly different ( $p < 0.001$ ) between groups; post-hoc tests indicated that STZ+10kHzSCS demonstrated a significantly ( $p = 0.02$ ) reduced firing rate in response to paw brush compared to STZ+ShamSCS (Figure 5A). Additionally, the Naïve group showed a statistically reduced firing rate ( $p < 0.03$ ) compared to all other groups.

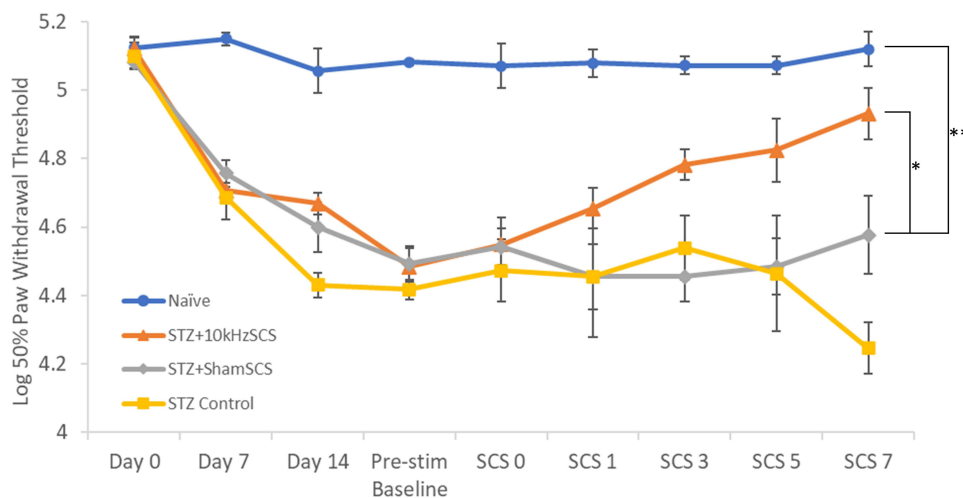


**Figure 3** Paw withdrawal thresholds for each experimental group over time. \*  $p < 0.05$ ; \*\*  $p < 0.01$ .

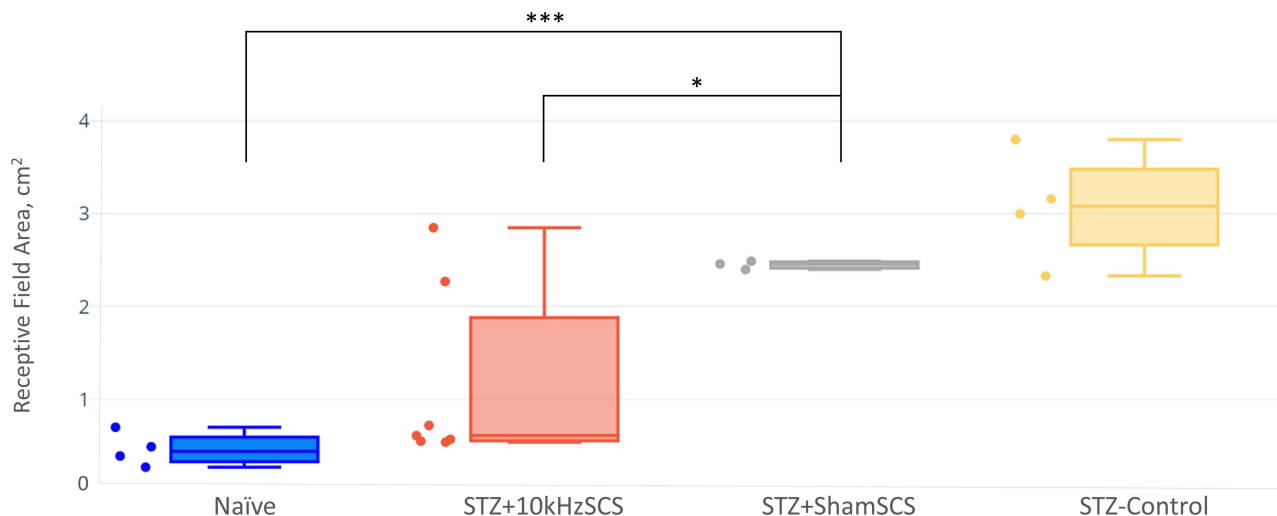


**Figure 4** Receptive field size of plantar surface of left hind paw for each experimental group. \*  $p < 0.05$ ; \*\*\*  $p < 0.001$ .

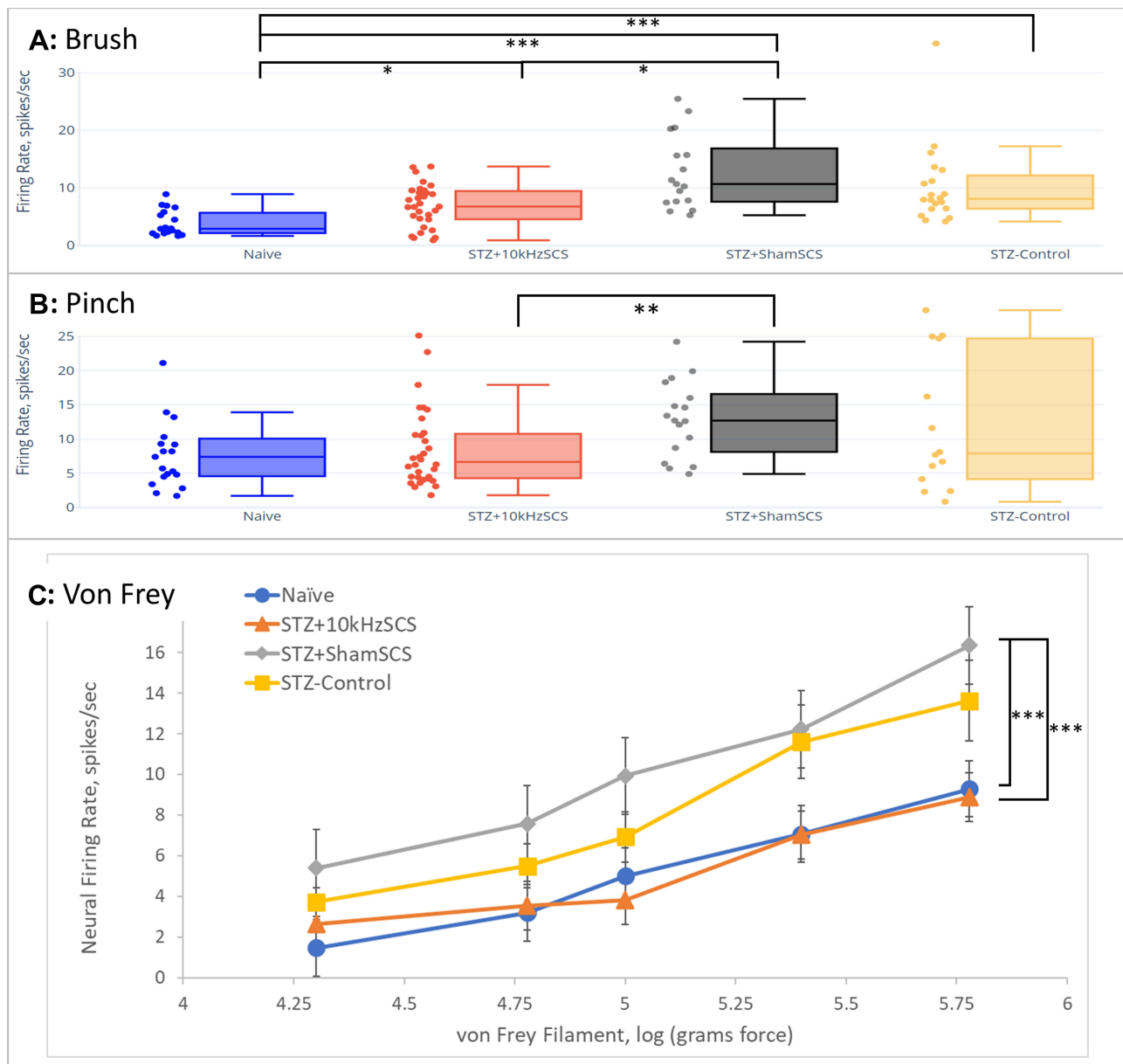


**Figure 5** Firing rate of dorsal horn neurons for each experimental group in response to (A) innocuous brush, (B) painful pinch, and (C) graded von Frey filament probing, of plantar surface of left hind paw. \*  $p < 0.05$ ; \*\*  $p < 0.01$ ; \*\*\*  $p < 0.001$ .

**Mechanosensitivity, Pinch:** The responses of neurons to application of a painful pinch to the plantar portion of the hind paw were significantly different ( $p = 0.003$ ) across groups (Figure 5B); post-hoc tests indicated that STZ+10kHzSCS demonstrated a significantly ( $p = 0.002$ ) reduced firing rate in response to painful pinch of the left hind paw.

**Mechanosensitivity, von Frey:** The neural response to increasing stiffness of vF filaments applied to the plantar portion of the paw was typically a monotonic increase in firing rate of dorsal horn neurons (Figure 5C). As in the behavioral data, for linear statistical analyses, we converted the grams-Force of vF measurements using a log transformation.<sup>24</sup> Two-way ANOVA revealed a statistically significant difference between groups ( $p < 0.001$ ) and filament stiffness ( $p < 0.001$ ); post-hoc *t*-Test comparisons with Bonferroni correction to STZ+ShamSCS indicated that STZ+10kHzSCS and Naïve groups were statistically different ( $p < 0.001$ ) from STZ+ShamSCS, while STZ-Control was not ( $p = 0.04$ ).

## Discussion

This work was inspired by recent clinical results demonstrating excellent pain relief in patients with diabetic peripheral neuropathy using 10 kHz SCS.<sup>10</sup> In prior preclinical studies of 10 kHz at clinically relevant intensities, different segmental effects on dorsal horn neurons were observed. Lee et al demonstrated, using SCS at 30% of MT, that 10 kHz, but not 1 kHz or 5 kHz, selectively activated inhibitory neurons in the superficial dorsal horn in rats and mice.<sup>15</sup> Also, Liao et al showed that 10 kHz at 30% of MT partially restored altered spinal glutamate processing in the dorsal horn of rodents.<sup>14</sup> Lee et al used “normal” animal models, while Liao et al employed spared nerve injury models. Thus, this present study represents the first investigations into the effects of clinically relevant 10 kHz SCS in diabetic animal models.

This study also differs critically in two respects from other prior studies of SCS in STZ diabetic pain models. First, the use of 10 kHz here is 20x higher than the highest frequency explored in this particular animal model. In STZ-model rodents, Pluijms et al demonstrated no frequency-dependent differences in paw withdrawal thresholds using frequencies ranging from 4 to 375 Hz.<sup>25</sup> Also, Van Beek et al reported that 500 Hz SCS showed a delayed response in paw withdrawal threshold improvements, different from the more immediate responses observed during the application of SCS at low (5 Hz) and medium (50 Hz) frequencies.<sup>26</sup> Second, we used stimulation amplitudes (30% of the SCS-driven motor threshold) that would not activate the dorsal columns and thus would not likely produce sensory paresthesia, as is observed in clinical applications of 10 kHz SCS.<sup>27</sup> Prior preclinical studies investigating the use of “paresthesia-based” SCS in the STZ diabetic model rat used amplitudes  $\geq 67\%$  of the motor threshold, understood to translate to strong dorsal column stimulation.<sup>22,23,28,29</sup> Thus, the mechanisms explored in this study would relate primarily to the effects of high kHz frequencies on non-dorsal column spinal neurons.

## STZ Model

In general, we found that our implementation of the STZ model of diabetic neuropathy generally agreed with the phenotype seen in the literature.<sup>16–18,30</sup> On average, in rats injected with STZ, blood glucose was clearly elevated to  $>270$  mg/dl by Day 7 and appeared to settle to  $>450$  mg/dl at Day 14 through to Day 28. Similarly, we saw a statistically significant reduction of approximately 13% in body weight over the experimental period compared to the Naïve group.

In a functional sense, clear disease responses were observed in the mechanical allodynia/vF testing, where all STZ-injected groups demonstrated statistically significant reduction of paw withdrawal threshold to approximately 88% of the Pre-SCS Baseline (~20 d post-STZ injection), in general agreement with similar preparations from the literature.<sup>22,23,26</sup> We infer from these responses that our model was appropriate for our assessments of possible therapeutic effects of 10 kHz SCS in an animal model of painful diabetic neuropathy.

## Behavioral

In the behavioral work, we observed recovery of the paw withdrawal threshold in the chronic 10 kHz SCS rats to within an average of 96% of both the Naïve group and the 10 kHz SCS pre-STZ Baseline values. The paw withdrawal threshold of the 10 kHz SCS group was statistically significantly improved compared to its own Pre-SCS Baseline, as well as compared to the STZ+ShamSCS group. One key difference in our study from previous preclinical investigations of SCS for PDN was the use of continuous 24 h/d SCS over a 1 w period, whereas the longest daily duration in the dorsal column stimulation for PDN investigations was 12h/d over a 4 w period.<sup>26</sup> This generally reflects clinical use models of the different types of SCS. 10 kHz SCS is paresthesia-free, which allows patients to run the stimulator continuously, especially important during the night, as the lack of paresthesia eliminates the concern for sleep-disturbing paresthesia intensity changes due to changing body position during supine/prone rest. In contrast, use of paresthesia-based SCS is more likely limited to awake hours, where the conscious patient can manage any intensity changes during activities of daily living.<sup>31,32</sup> In Van Beek et al, statistically significant improvement in the paw withdrawal threshold was only observed after 4 w of 12 h/d SCS, whereas we observed significant improvements after one week.<sup>28</sup> This observed different time-course of effect further underscores a likely different mechanism of action for 10 kHz SCS. Additionally,



the progressive improvement we observed in the paw withdrawal threshold over the 7 d period of 10 kHz SCS aligns with clinical observations, where 10 kHz SCS is known to provide pain relief several days after activation.<sup>25</sup>

## Electrophysiology

We observed that 10 kHz SCS improved several electrophysiologic metrics of neural hyperexcitability. First, neural responses to innocuous stimuli such as brush and low-force vF probing were shown to be elevated in the STZ-Control and STZ+ShamSCS, suggesting that our STZ model reflected a state of central sensitization, in keeping with the literature.<sup>33</sup> The STZ+10kHzSCS animal group showed statistically significant reductions in responses compared to the STZ+ShamSCS group for both light brushing and vF stimuli, which would be analogous to a reduction in clinical allodynia.<sup>34</sup>

Similarly, neural responses to presumed painful external stimuli to the paw, including high-force vF and pinch (preclinical analogs to hyperalgesia in patients), were also significantly reduced in the STZ+10kHzSCS group as compared to the STZ+ShamSCS group.<sup>35,36</sup> These results align reasonably well with the behavioral response in each group, suggesting that the 10 kHz SCS was responsible for reducing dorsal horn hyperexcitability to both innocuous as well as painful stimuli.

Expansion of the receptive field of dorsal horn neurons is a known phenomenon in neuropathic as well as diabetic animal models.<sup>20,31,37</sup> In the context of pain, such expansion is believed to be a marker of spinal central sensitization and represents a means for increased pain experience by amplifying pain through increased spatial summation.<sup>22</sup> In keeping with the other electrophysiologic metrics of pain, we observed that the STZ+10kHzSCS group had a statistically significant reduction in the receptive field compared to the STZ+ShamSCS group, suggesting reduction in central sensitization.

Expansion of the receptive field may also relate to compromised sensory processing. If the receptive field is expanded, spatial acuity would be decreased, and this might appear as a sensory deficit.<sup>38</sup> A clinical measure related to the receptive field is two-point discrimination, a measure of spatial/tactile acuity.<sup>39</sup> Chronic pain patients, such as those with CRPS and non-neuropathic back pain do show altered two-point discrimination.<sup>40,41</sup> Periasamy et al demonstrated that two-point discrimination distance was increased in diabetic patients.<sup>42</sup> This could reflect either peripheral or central dysfunction, though the relatively equal bilateral increase they observed may more likely point to a central deficit. Based on our observations here, we hypothesize that if RF field is reduced/normalized via 10 kHz SCS, then this could partially explain why anecdotal sensory improvements were observed in PDN patients using 10 kHz SCS.<sup>10</sup>

## Conclusion

Low intensity 10 kHz SCS resulted in behavioral and electrophysiological outcomes reflective of pain reduction in a commonly used rodent model of painful diabetic neuropathy. This work underscores the clinical findings of significant and robust pain relief in PDN patients using paresthesia-free 10 kHz SCS, and lays the groundwork for further exploration of newer mechanisms not dependent upon dorsal column activation.

## Abbreviations

BG, blood glucose; cm, centimeter(s); d, day(s); dl, deciliter; DPN, diabetic peripheral neuropathy; g, gram; Hz, hertz; h, hour(s); IP, intraperitoneal; kg, kilograms; kHz, kilohertz; m, meter(s); um, micrometer(s); mg, milligrams; mm, millimeter(s); m, minute(s); MT, motor threshold; PDN, painful diabetic neuropathy; s, second(s); SNRI, selective norepinephrine reuptake inhibitors; SCS, spinal cord stimulation; STZ, streptozotocin; vF, von Frey; w, week(s).

## Data Sharing Statement

The data, analytic methods, and study materials for this trial may be made available to other researchers in accordance with the policies of Nevro Corp.

## Ethics

All experimental procedures were carried out in accordance with the National Institute of Health Guide for the Care and Use of Laboratory Animals and approved by the Animal Care Committee at Explora BioLabs (San Diego, CA), protocol number EB20-016-001.

## Consent to Publish

All authors provide consent to the Journal of Pain Research to publish all content contained within this article.

## Acknowledgments

Jean-Louis Marchal was involved in the statistical analysis of the data as a paid consultant. Ethan Pham was involved in the data collection, discussion, and analysis as a paid laboratory assistant.

## Author Contributions

All authors made substantial contributions to conception and design, acquisition of data, or analysis and interpretation of data; took part in drafting the article or revising it critically for important intellectual content; agreed to submit to the current journal; gave final approval of the version to be published; and agree to be accountable for all aspects of the work.

## Funding

This work was financially supported by Nevro Corporation.

## Disclosure

Dong Wang, Kwan Yeop Lee, Dongchul Lee, Zachary B Kagan, and Kerry Bradley are full-time employees of Nevro Corporation and were involved in the study design, data collection and analysis, and preparation of the manuscript. Dong Wang reports salary and stock options from Nevro during the conduct of the study. Zachary B Kagan reports salary and stock options during the conduct of the study. Kwan Yeop Lee reports salary from Nevro outside the submitted work. Dongchul Lee reports salary from Nevro during the conduct of the study. Mr Kerry Bradley reports salary, stock, and stock options for Nevro during the conduct of the study. The authors report no other potential conflicts of interest for this work.

## References

1. Pop-Busui R, Boulton AJ, Feldman EL, et al. Diabetic neuropathy: a position statement by the American Diabetes Association. *Diabetes Care*. 2017;40:136–154.
2. Schmader KE. Epidemiology and impact on quality of life of postherpetic neuralgia and painful diabetic neuropathy. *Clin J Pain*. 2002;18:350–354.
3. Bril V, England J, Franklin GM, et al. American Academy of Neurology; American Association of Neuromuscular and Electrodiagnostic Medicine; American Academy of Physical Medicine and Rehabilitation. Evidence-based guideline: treatment of painful diabetic neuropathy: report of the American Academy of Neurology, the American Association of Neuromuscular and Electrodiagnostic Medicine, and the American Academy of Physical Medicine and Rehabilitation. *Neurology*. 2011;76:1758–1765.
4. Finnerup NB, Attal N, Haroutounian S, et al. Pharmacotherapy for neuropathic pain in adults: a systematic review and meta-analysis. *Lancet Neurol*. 2015;14:162–173.
5. Yang M, Qian C, Liu Y. Suboptimal treatment of diabetic peripheral neuropathic pain in the United States. *Pain Medicine*. 2015;16:2075–2083.
6. Tesfaye S, Watt J, Benbow SJ, Pang KA, Miles J, MacFarlane IA. Electrical spinal-cord stimulation for painful diabetic peripheral neuropathy. *Lancet*. 1996;348:1698–1701.
7. de Vos CC, Meier K, Zaalberg PB, et al. Spinal cord stimulation in patients with painful diabetic neuropathy: a multicentre randomized clinical trial. *Pain*. 2014;155:2426–2431.
8. van Beek M, Slangen R, Schaper NC, et al. Sustained treatment effect of spinal cord stimulation in painful diabetic peripheral neuropathy: 24-month follow-up of a prospective two-center randomized controlled trial. *Diabetes Care*. 2015;38:e132–e134.
9. van Beek M, Geurts JW, Slangen R, et al. Severity of neuropathy is associated with long-term spinal cord stimulation outcome in painful diabetic peripheral neuropathy: five-year follow-up of a prospective two-center clinical trial. *Diabetes Care*. 2018;41:32–38.
10. Petersen EA, Stauss TG, Scowcroft JA, et al. Effect of high-frequency (10-kHz) spinal cord stimulation in patients with painful diabetic neuropathy: a randomized clinical trial. *JAMA Neurol*. 2021;1:24.
11. Kapural L, Yu C, Doust MW, et al. Novel 10-kHz high-frequency therapy (HF10 therapy) is superior to traditional low-frequency spinal cord stimulation for the treatment of chronic back and leg pain: the SENZA-RCT randomized controlled trial. *Anesthesiology*. 2015;123:851–860.
12. Kapural L, Yu C, Doust MW, et al. Comparison of 10-kHz high-frequency and traditional low-frequency spinal cord stimulation for the treatment of chronic back and leg pain: 24-month results from a multicenter, randomized, controlled pivotal trial. *Neurosurgery*. 2016;79:667–677.
13. Tieppo Francio V, Polston KF, Murphy MT, Hagedorn JM, Sayed D. Management of Chronic and Neuropathic Pain with 10 kHz Spinal Cord Stimulation Technology: summary of Findings from Preclinical and Clinical Studies. *Biomedicine*. 2021;9:644.
14. Liao WT, Tseng CC, Chia WT, Lin CR. High-frequency spinal cord stimulation treatment attenuates the increase in spinal glutamate release and spinal miniature excitatory postsynaptic currents in rats with spared nerve injury-induced neuropathic pain. *Brain Res Bull*. 2020;164:307–313.
15. Lee KY, Bae C, Lee D, et al. Low-intensity, kilohertz frequency spinal cord stimulation differently affects excitatory and inhibitory neurons in the rodent superficial dorsal horn. *Neuroscience*. 2020;428:132–139.
16. Furman BL. Streptozotocin-induced diabetic models in mice and rats. *Curr Protocols Pharmacol*. 2015;70:5–47.

17. Goyal SN, Reddy NM, Patil KR, et al. Challenges and issues with streptozotocin-induced diabetes—a clinically relevant animal model to understand the diabetes pathogenesis and evaluate therapeutics. *Chem Biol Interact.* 2016;244:49–63.
18. Calcutt NA. Modeling diabetic sensory neuropathy in rats. *Methods Mol Med.* 2004;99:55–65.
19. Gonzalez-Cano R, Boivin B, Bullock D, Cornelissen L, Andrews N, Costigan M. Up-down reader: an open source program for efficiently processing 50% von Frey thresholds. *Front Pharmacol.* 2018;9:433.
20. Mills C, LeBlond D, Joshi S, et al. Estimating efficacy and drug ED50's using von Frey thresholds: impact of Weber's law and log transformation. *The Journal of Pain.* 2012;13:519–523.
21. Fischer TZ, Tan AM, Waxman SG. Thalamic neuron hyperexcitability and enlarged receptive fields in the STZ model of diabetic pain. *Brain Res.* 2009;1268:154–161.
22. Tan AM, Samad OA, Dib-Hajj SD, Waxman SG. Virus-mediated knockdown of Nav1.3 in dorsal root ganglia of STZ-induced diabetic rats alleviates tactile allodynia. *Molecular Medicine.* 2015;21:544–552.
23. Lee KY, Ratté S, Prescott SA. Excitatory neurons are more disinhibited than inhibitory neurons by chloride dysregulation in the spinal dorsal horn. *Elife.* 2019;8:e49753.
24. Chaplan SR, Bach FW, Pogrel JW, Chung JM, Yaksh TL. Quantitative assessment of tactile allodynia in the rat paw. *J Neurosci Methods.* 1994;53:55–63.
25. Pluijms WA, van Kleef M, Honig WM, Janssen SP, Joosten EA. The effect of spinal cord stimulation frequency in experimental painful diabetic polyneuropathy. *Eur J Pain.* 2013;17:1338–1346.
26. van Beek M, van Kleef M, Linderth B, Van Kuijk SM, Honig WM, Joosten EA. Spinal cord stimulation in experimental chronic painful diabetic polyneuropathy: delayed effect of high-frequency stimulation. *Eur J Pain.* 2017;21:795–803.
27. Russo M, Van Buyten JP. 10-kHz high-frequency SCS therapy: a clinical summary. *Pain Medicine.* 2015;16:934–942.
28. van Beek M, Hermes D, Honig WM, et al. Long-term spinal cord stimulation alleviates mechanical hypersensitivity and increases peripheral cutaneous blood perfusion in experimental painful diabetic polyneuropathy. *Neuromodulation.* 2018;21:472–479.
29. Dietz BE, Muga D, Vuong QC, Obara I. Electrically evoked compound action potentials in spinal cord stimulation: implications for preclinical research models. *Neuromodulation.* 2021.
30. Kou ZZ, Li CY, Hu JC, et al. Alterations in the neural circuits from peripheral afferents to the spinal cord: possible implications for diabetic polyneuropathy in streptozotocin-induced type 1 diabetic rats. *Front Neural Circuits.* 2014;8:6.
31. North RB, Ewend MG, Lawton MT, Piantadosi S. Spinal cord stimulation for chronic, intractable pain: superiority of “multi-channel” devices. *Pain.* 1991;44(2):119–130.
32. Amirdeflan K, Yu C, Doust MW, et al. Long-term quality of life improvement for chronic intractable back and leg pain patients using spinal cord stimulation: 12-month results from the SENZA-RCT. *Quality Life Res.* 2018;27:2035–2044.
33. Chen SR, Pan HL. Hypersensitivity of spinothalamic tract neurons associated with diabetic neuropathic pain in rats. *J Neurophysiol.* 2002;87:2726–2733.
34. Sandkuhler J. Models and mechanisms of hyperalgesia and allodynia. *Physiol Rev.* 2009;89:707–758.
35. Kostek M, Polaski A, Kolber B, Ramsey A, Kranjec A, Szucs K. A protocol of manual tests to measure sensation and pain in humans. *JoVE.* 2016;1:e54130.
36. Pfau DB, Haroun O, Lockwood DN, et al. Mechanical detection and pain thresholds: comparability of devices using stepped and ramped stimuli. *Pain Reports.* 2020;5:356.
37. Cook AJ, Woolf CJ, Wall PD, McMahon SB. Dynamic receptive field plasticity in rat spinal cord dorsal horn following C-primary afferent input. *Nature.* 1987;325:151–153.
38. Greenspan JD, Bolanowski SJ. The psychophysics of tactile perception and its peripheral physiological basis. In: Kruger L, editor. *Pain and Touch.* 1st ed. Cambridge, MA: Academic Press; 1996:25–103.
39. Johnson KO, Phillips JR. Tactile spatial resolution. I. Two-point discrimination, gap detection, grating resolution, and letter recognition. *J Neurophysiol.* 1981;46:1177–1192.
40. Pleger B, Tegenthoff M, Ragert P, et al. Sensorimotor returning in complex regional pain syndrome parallels pain reduction. *Ann Neurol.* 2005;57:425–429.
41. Catley MJ, O'Connell NE, Berryman C, Ayhan FF, Moseley GL. Is tactile acuity altered in people with chronic pain? A systematic review and meta-analysis. *The Journal of Pain.* 2014;15:985–1000.
42. Periyasamy R, Manivannan M, Narayanamurthy VB. Changes in two point discrimination and the law of mobility in diabetes mellitus patients. *J Brachial Plex Peripher Nerve Inj.* 2008;3:1–6.